



Investigation of the Surface Grooves Effect in Hydrodynamic Lubrication

Experimentally

Muhannad Mohsen Mrah^{1*}, Ammar S. Hamid Merza¹

¹Mechanical Engineering Department, University of Technology, Baghdad-Iraq

* me.19.23@grad.uotechnology.edu.iq

Received:	8/1/2022	Accepted:	2/2/2022	Published:	14/2/2022
-----------	----------	-----------	----------	------------	-----------

Abstract

This research aims to study the effect of rectangular slots on the pressure distribution in an inclined slider bearing. The pressure gradient in a one-dimensional fluid sheet was theoretically calculated using Reynolds' equation. The practical results were compared by the tilted sliding bearing, where the researcher manufactured and developed the device by adding pressure sensors along the pads. Four pads with varied slot widths (3, 5, and 8mm) and a depth of 2mm were created: one without grooves and three with rectangular grooves. The research examined various factors, including sliding velocities, pad inclination values, and oil temperatures. The conclusions indicate that the flat model's pressure distribution was significantly superior to the slot models by percentages of 0.5%, 4.2%, and 14%, respectively. One significant conclusion for models with slots was that as the inclination increases, the maximum hydrodynamic pressure began to move towards the pad's beginning. Thus, grooved versions can be employed in applications needing less load and weight. Experimental comparisons between the present and previous work have been made (just in behaviors). The comparison sample was flat; the results indicated that sensors produced higher pressure levels than manometer tubes under the same operating conditions.

Keywords: Tribology, Surface grooves, Inclined Bearing, Hydrodynamic Lubrication, and Pressure distribution.

Introduction

The wide range of mechanical applications with interacting surfaces and increased industrial competition for improved performance has led to increased attention to research in the science of friction, wear, and lubrication, i.e., tribology [1]. Many machine components, e.g., bearings, gears, piston rings, and breaks, consist of parts that operate by rubbing against each other [2]. With extensive applications of slider bearings in mechanical devices, investigations associated with their design and performance optimization have been given privilege. The current industrial requirements include increased load carrying capacity, lower friction, and lower power consumption. To increase the bearing performance in different machine elements during lubrication, e.g., slider bearings and roller bearings, it is essential to find the optimum slider bearings such as plane surfaces, step, composite, inclined, etc. Wherein this research, slider bearings with grooved shapes of pads are investigated experimentally. Slider bearings are widely used in engineering applications such as machine tools, steam turbines, gas turbines,



piston rings, etc. (for their load-carrying capacity, excellent stability, and durability) [3]. Some researchers analyzed slider bearings for different purposes using numerical techniques, treating the analyzed film thickness as the slider bearing shape function. So, manufacturing a slider bearing shape is sometimes challenging to match with the numerical shape, so the approach shape function can be obtained using curve fitting techniques. However, there is inevitably some error between the numerical shape and the curve-fitting shape function. The selection of a slider bearing is governed by many considerations, where some designers have analyzed slider bearings with various shapes. Generally, bearing designers usually try to select design variables within constraints by a trial and error method using many design charts obtained from bearing characteristic analysis. However, these approximated results do not necessarily produce the optimum solutions. Hence, the optimum design for slider-bearing shapes for different purposes has become an essential and exciting topic in recent years.

Recently, surface texturing has been used to improve the tribological characteristics of mechanical components [4]-[6]. Generally, the primary functions of surface texturing are to act as traps for wear debris [7], to control adhesion and stiction [8], to provide reservoirs for improved lubricant retention [9], and to generate hydrodynamic pressure to increase load-carrying capacity [10,11], among others. With these capabilities, it is not surprising that surface texturing is widely used in a variety of fields, including mechanical seals [12, 13], piston rings [14], thrust bearings [15, 16], and journal bearings [17].

Objectives

The previous scientific literature that discusses the combined effects of pad surface profile and pad geometry assumes flat pads with no rectangular slots in the surfaces. The goal of reducing friction and the desire to get the highest load capacity in the operating conditions of tilting-pad thrust bearings resulted in the following research questions:

The first research question: Due to the wide applications of sliding bearings in mechanical devices, great importance is given to the study of their design. So what are the effects of surface grooves on fluid pressure distribution?

The second research question: Is it possible to achieve performance improvements, i.e., a lower friction coefficient and higher load-carrying capacity, by applying features like rectangular slots to the surfaces of the bearing pads?

The shape of sliding bearings is subject to many considerations. Usually, bearing designers try to select design variables within work constraints through trial and error methods, using design schemes resulting from analysis of bearing characteristics. This method often produces unconvincing results and does not give the optimal design solution. Thus, the optimal design of sliding bearing shapes has become an essential and exciting topic in recent years.

In this research, it is essential to obtain the optimal shape of inclined bearings that meets the desired ambition of obtaining the highest load capacity and the lowest friction, thus obtaining the lowest energy consumption in the machine during lubrication.

Experimental Apparatus

The system consists of a plane aluminum slider, 12.5cm^2 , whose dimensions are placed precisely in proportion to the movable belt, which carries a thick oil film. Figure 1. shows a diagram of the device used, consisting of two rotating cylinders (A, B) connected by an oil conveyor belt. The cylinder (A) is driven by an electric motor through which the cylinder rotation speed can be controlled and thus the linear velocity of the conveyor belt. Models with the exact dimensions as the slider but a thickness of 4mm can be installed in the lower area of the slider. It contains pressure gauge holes attached to it, plastic tubes that transfer the oil pressure to the sensors to measure the oil pressure inside the sample, and these tubes are longitudinally distributed. To calculate the change in pressure resulting from the trapping of oil between the moving belt and the model tilted at a certain angle and cross tubes to indicate the balance and level of the device, the oil flows from (C) to region (D). The clearance between the belt and the sample is controlled by a micrometer at the edge (C, D), and the device is placed in a basin, part of which is filled with oil.

Note: The researcher manufactured and developed the device at home, where it will be dedicated to the fluid laboratories at the University of Technology.

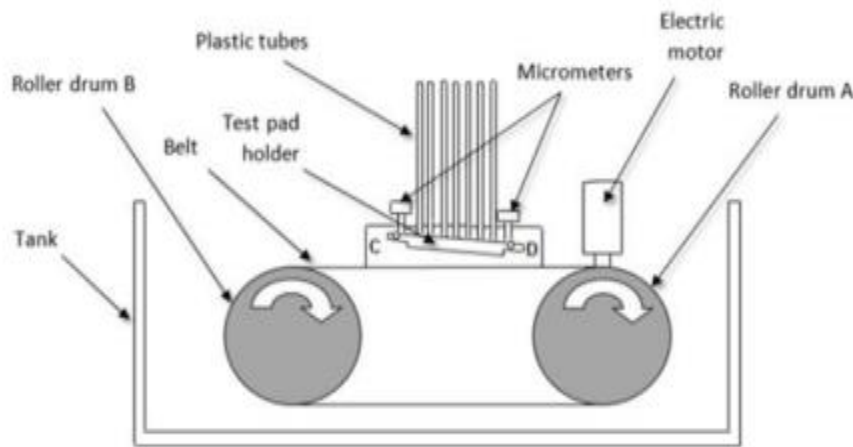


Figure 1: Schematic of the experimental apparatus.

Two micrometers are used to determine the clearance between the slider and the belt. They are positioned parallel to the leading and trailing edges of the slider. One of these micrometers was fixed to the lead edge, while the other was fixed to the trailing edge. Thirteen pressure sensors attached to the slider indicate the amount of oil pressure created by the slider and the moving belt via plastic tubes. Seven of these sensors are evenly spaced along the slider's axis in the direction of movement. At the same time, another group is transversely located in a plane roughly parallel to the point where the oil's maximum pressure is supposed to occur [18]. The devices used with the additional instruments are depicted in Figure 2.



Figure 2: Test apparatus.

Materials and Method

Materials

Aluminum was used as the metal for the produced models. This metal was chosen for its availability and simplicity of installation on the equipment. The metal was chopped into squares (12.5 cm^2) to match the models (4). The thickness of the manufactured models is 4 mm. A CNC machine was used to create rectangular grooves on the models. Four pads were manufactured, one without slots and three with rectangular grooves (orienting the grooves in the direction of the oil flow) and varying slot widths (3, 5, and 8mm) and a depth of 2mm, as shown in Figure 3. The models must be identical in size to the holes in the equipment used, have the same diameter, and have the same number of holes (13). These holes are placed next to the pad's holes to allow oil to flow through the pipes to measure the oil pressure.



Figure 3: Flat and Slots models



Method

The Reynolds equation describes the change of lubricating pressure in a bearing. The most popular lubricated slider bearing is the inclined plane pad, which demonstrates how the Reynolds equation may be used for slider bearings (where this type has been studied in this research). The complete equation is complicated to solve. Still, a reduced form will be utilized in the first instance by making several derivational assumptions and using the equilibrium of a tiny element to derive the Reynolds equation in one dimension [19].

Assumptions

We make the following assumptions:

1. Body forces are disregarded, which implies that no external force field, such as gravitational or magnetic forces, acts on the lubricant.
2. The fluid is incompressible and Newtonian (obey Newton's law of viscosity).
3. The flow is laminar.
4. The bearing is infinitely vast.
5. The viscosity of the film remains constant throughout its thickness. This is undoubtedly not true, but it adds a layer of complication if not accepted [19].

Reynolds' Equation Applied to Sliding Bearings:

The following equation was developed to express the change in pressure along a converging fluid film in terms of the velocity gradient across the film [19]:

$$\frac{dP}{dx} = \eta \frac{d^2u}{dy^2} \quad (1)$$

$$\text{or } \frac{d^2u}{dy^2} = \frac{1}{\eta} \frac{dP}{dx} \quad (2)$$

Integrating Eq. (2) twice with respect to y gives:

$$u = \int \frac{1}{\eta} \frac{dP}{dx} y \, dy + C_1 \, dy = \frac{1}{2\eta} \frac{dP}{dx} y^2 + C_1 y + C_2 \quad (3)$$

The constants of integration C_1 and C_2 may be evaluated from the boundary conditions:

1. $u = U$ when $y = 0$
2. $u = 0$ when $y = h$

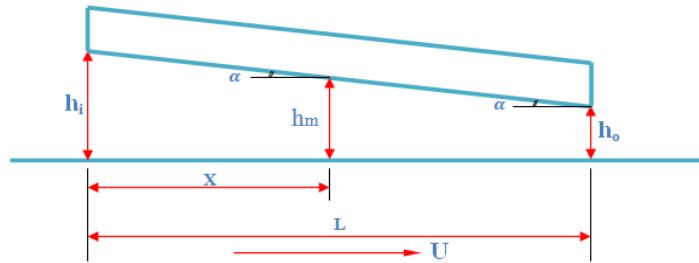


Figure 4. Geometry of a linear pad bearing.

From condition (1) it follows that $C_2 = U$ and from condition (2)

$$C_1 = -\frac{1}{2\eta} \frac{dP}{dx} h - \frac{U}{h}$$

By introducing the values of these constants into Eq. (3), it becomes:

$$u = \frac{1}{2\eta} \frac{dP}{dx} (y^2 - hy) + U \frac{h-y}{h} \quad (4)$$

The first component in the right-hand member of Eq. (4) denotes a parabolic distribution of velocity caused by the pressure-driven flow in the film. The second component in Eq. (4)'s right-hand member illustrates a linear distribution of velocity caused by the relative motion of the two surfaces.

The expression for the volume of fluid flowing through the bearing By using the above assumptions and defining (Q) as the volume of fluid flowing in a unit of time:

$$Q = \int_0^h u \, dy$$

By substituting the value of u from Eq. (4) and integrating, the equation for (Q) becomes,

$$Q = \frac{Uh}{2} - \frac{h^3}{12\eta} \frac{dP}{dx}$$

For an incompressible fluid, the flow is the same for all cross sections of the film, or

$$\frac{dQ}{dx} = 0$$

Therefore,

$$\frac{dQ}{dx} = \frac{U}{2} \frac{dh}{dx} - \frac{d}{dx} \left(\frac{h^3}{12\eta} \frac{dP}{dx} \right) = 0$$



$$\frac{d}{dx} \left(h^3 \frac{dP}{dx} \right) = 6 \eta U \frac{dh}{dx} \quad (5)$$

This is the one-dimensional Reynolds' equation for the pressure gradient in a converging fluid film, which is ignored by side leakage (flow in the z-direction).

Note: This general formula is used exclusively for theoretical and experimental comparisons of flat pads. In the case of grooved pads, only experimental results are discussed.

1. Pressure and load capacity distributions

Integrating Eq. (5) twice with respect to X gives [20]:

$$P = \frac{6 \eta U L}{h_0^2 (K-1)} \left[\frac{1}{h^*} - \frac{h_i}{h^{*2} (h_i + h_o)} - \frac{h_o}{h_i + h_o} \right]$$

Substituting ($h_i = K h_o$) in above equation gives:

$$P = \frac{6 \eta U L}{h_0^2} \left(\frac{K-1}{K+1} \frac{\frac{X}{L} (1 - \frac{X}{L})}{[K - (K-1) \frac{X}{L}]^2} \right) \quad (6)$$

Further integration of Eq. (6) yields the sliding bearing's normal load capacity per unit width:

$$\frac{W}{B} = \int_{x=0}^{x=L} P dx \quad (7)$$

The load bearing capacity equation becomes:

$$W = \frac{6 \eta U L^2 B}{h_0^2} \frac{1}{(K-1)^2} \left(\log_e K - \frac{2(K-1)}{K+1} \right) \quad (8)$$

2. Shear stress in hydrodynamic film

To evaluate the shear stress along the length of the bearing at the lower surface, the definition of Newtonian viscosity and Eq. (4) is used to get:

$$\tau_o = -\frac{h}{2} \frac{dP}{dx} - \frac{\eta U}{h} \quad (9)$$

Moreover, the shear stress at the upper surface is:

$$\tau_h = \frac{h}{2} \frac{dP}{dx} - \frac{\eta U}{h} \quad (10)$$



3. Friction force

Friction is the resistance to motion that exists between two solid bodies as one slides over the other. The resistive force perpendicular to the direction of motion is referred to as the "friction force". Even such negligible frictional forces result in energy waste and subsequent loss of machine efficiency. As a result, the designer's goal is often to minimize frictional forces. The frictional force is calculated using the following equation:

$$F = \int_0^L \tau \, dx \quad (11)$$

The friction force on the lower surface is

$$F_o = \frac{\eta U L B}{h_o} \left[\frac{4 \log_e K}{K-1} - \frac{6}{K+1} \right] \quad (12)$$

$$F_h = \frac{\eta U L B}{h_o} \left[\frac{2 \log_e K}{K-1} - \frac{6}{K+1} \right] \quad (13)$$

4. Coefficient of

It is known that

$$\mu = \frac{F}{W} \quad (14)$$

Substituting for W and F and simplification the above equation yields:

$$\mu = \frac{h_o}{L} (K-1) \left[\frac{2(K+1) \log_e K - 3(K-1)}{3(K+1) \log_e K - 6(K-1)} \right] \quad (15)$$

Experimental Calculations

The seven pressure sensors are tested with a constant belt speed for a range of film ratios, with the film thickness h_o at the trailing edge remaining constant while the film thickness h_i at the leading edge is gradually increased. The following are the corresponding calculations for a few of these tests [20]:

Table 1: List of parameters used in experimental calculations.

Models	flat
Type oil	Bright stock
Temperature	35 °C
Film ratio K (h_i / h_o)	2
Pad length (L)	0.125 m
Belt length	1.25 m
Sliding velocity	0.1 m/s
Density	900 kg/m ³
Viscosity of oil at T=35 °C	395 cSt

Generally, kinematic viscosity is expressed in centistokes; the relationship between viscosity (η) expressed in centistokes and in SI units is as follows:



$$v = (cSt) \times 10^{-6} \quad \text{m}^2/\text{s}$$

Given that kinematic viscosity is defined as (viscosity)/(density), the following may be written:

$$\eta = \rho v = \rho (cSt) 10^{-6} \quad \text{kg/ms}$$

- a) The pressure was calculated using Eq. (6).

$$P = \frac{6 \eta U L}{h_0^2} \left(\frac{K-1}{K+1} \frac{X}{L} (1 - \frac{X}{L}) \right) \left[K - (K-1) \frac{X}{L} \right]^2$$

Table 2: List of simple calculations

station	1	2	3	4	5	6	7
P(practical) pa	230	736	1393	2157	2835	3240	3160
P(theoretical)pa	329	985	1943	2827	3565	4060	4005

Note: Through the above table, it is possible to calculate the error rate between the theoretical and experimental parts, as the error rate is estimated at about 23%. The presence of such a percentage is due to the natural leakage of oil from both sides of the pad, in addition to the vibrations emanating from the motor, as well as the design of the pad (roughness and texture).

- b) The load capacity was calculated using Eq. (8).

$$W = \frac{6 \eta U L^2 B}{h_0^2} \frac{1}{(K-1)^2} \left(\log_e K - \frac{2(K-1)}{K+1} \right)$$

$$W = \frac{6 * 0.33 * 0.1 * (0.125)^2 * 0.125}{(0.0005)^2} \frac{1}{(2-1)^2} \left(\log_e 2 - \frac{2(2-1)}{2+1} \right)$$

$$W = 40.962 \text{ N}$$

- c) The coefficient of friction was calculated by using Eq. (15).

$$\mu = \frac{h_0}{L} (K-1) \left[\frac{2(K+1) \log_e K - 3(K-1)}{3(K+1) \log_e K - 6(K-1)} \right]$$

$$\mu = \frac{0.0005}{0.125} (2-1) \left[\frac{2(2+1) \log_e 2 - 3(2-1)}{3(2+1) \log_e 2 - 6(2-1)} \right]$$

$$\mu = 0.01945$$

increase the volume enclosed between the pad and the belt, requiring a more significant amount of oil

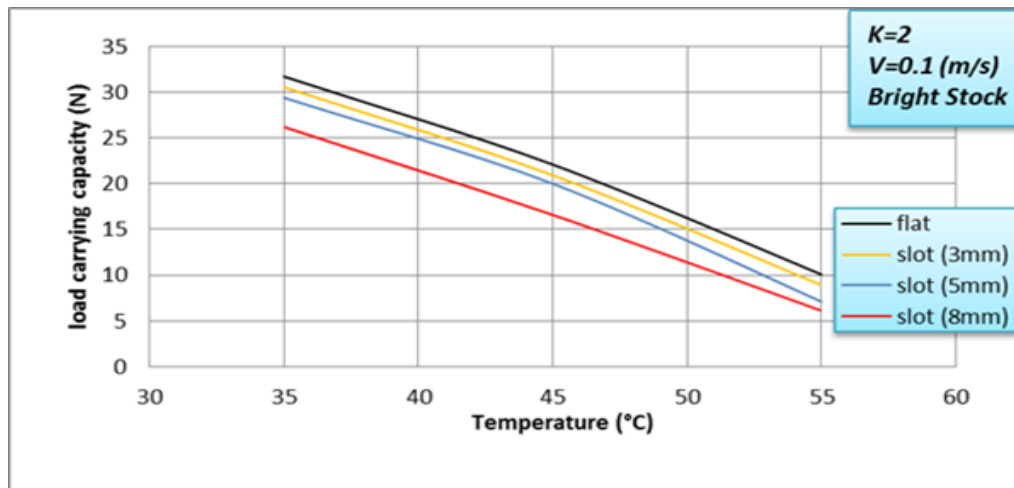


Figure 6: Relation between load capacity and temperature.

3. Effect of an inclination on the load-carrying capacity

The relationship between the inclination of the pad and the load-carrying capacity is depicted in Figure (7). The researchers observe that as the inclination increases, the load-carrying capacity decreases (inverse proportion). This is because the higher the inclination value, the more volume is constrained between the pad and the belt. As a result, the oil pressure is reduced (constant flow rate) in comparison to the flat pad. In the case of grooved pads, the presence of grooves increases the value of K , resulting in a more significant decrease in pressure. When the value of (K) is between (2-2.5), the maximum increase in (W) occurs, and then the value of (W) steadily decreases as the value of (K) increases. This is more accurate than what Gropper et al. recommended in their review (The highest load capacity is obtained whenever the value of the inclination of the cushion is close to zero) [23].

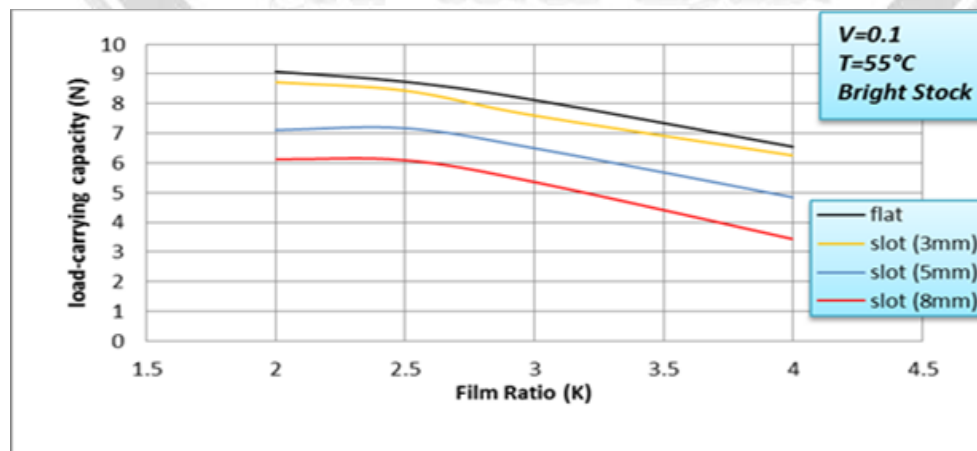


Figure 7: Relation between load capacity and film ratio.

generated on the pad surface at the trailing edge. Because the peak pressure is somewhat towards the trailing edge, the maximum pressure values are situated closer to the trailing edge.

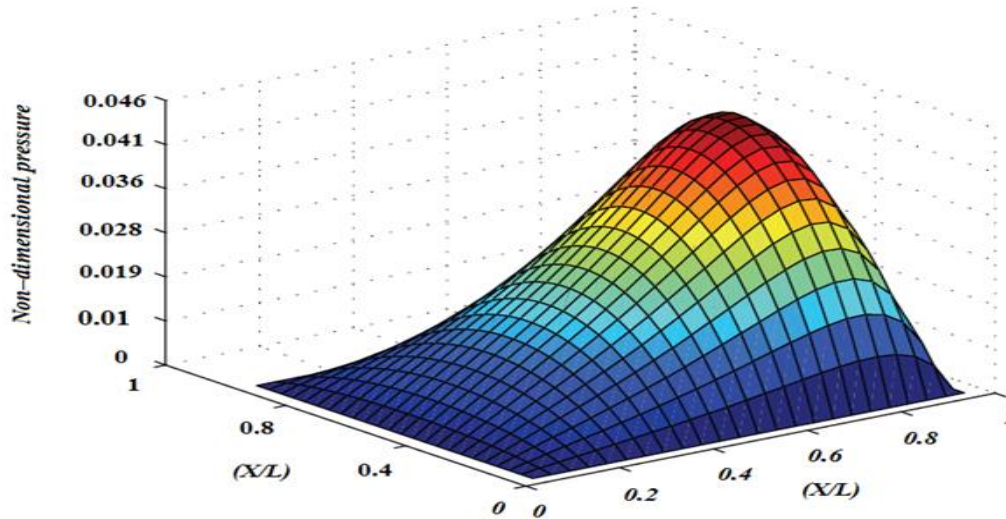


Figure 9: Non-dimensional pressure distribution with and circumferential directions.

5. Comparison between the present work and the previous work

The current study was evaluated in comparison to previous studies [21]. This comparison made use of a flat sample. In the current work, pressure sensors were used, whereas in the previous work, manometer tubes were used. As illustrated in Figure 10, the current work's pressure distribution is greater than it was at the previous work (but with the same behavior). This is because the sensors take readings directly from the pad's bottom surface. Previously, readings were obtained by observing the liquid level inside the manometer tubes, as the liquid inside the tubes has a different density than the liquid beneath the pad's surface due to the temperature difference between the oil and the surrounding environment. Due to the fact that temperature differences affect fluid density, the majority of research involving the pressure distribution in a sliding inclined bearing should pay close attention to this factor.

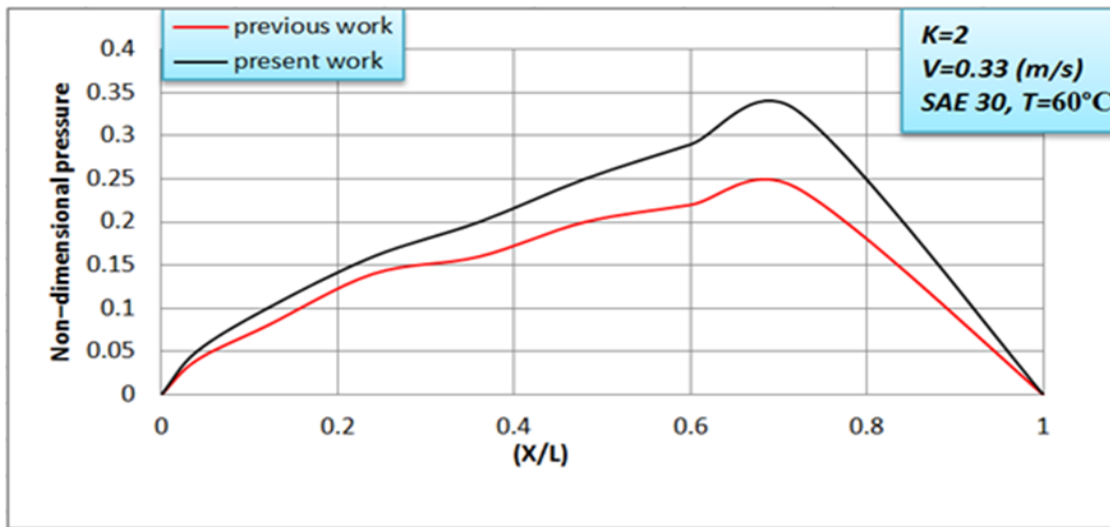


Figure 10: Comparison between the present work and the previous work.

Conclusions

The following conclusions may be inferred from the current study based on the examination of the findings: The pressure distribution is better when a flat model is utilized instead of a groove model under the identical operating conditions. The pressure distribution has been raised at (groove width of 3mm) greater than the increase at (groove width of 3mm) for grooved models (groove width of 5mm and 8mm). With percentages of 0.38%, 4.63%, and 17.37%, respectively, the flat model's coefficient of friction is lower than the groove models' coefficient of friction. The greatest load-carrying capacity of flat and groove models was in the film ratio (K) of 2 to 2.5, with the load capacity of the flat model outnumbering the load capacity of the groove models by 0.5%, 4.27%, and 14.66%, respectively. When the belt speed is increased, regardless of the test model, the pressure distribution improves. One important finding for grooved models is that as the inclination rises, the maximum load capacity approaches the center of the pad, enabling grooved versions to be employed in applications with lower load and weight requirements.

Nomenclature

Symbol	Description	Unit
B	Pad width	m
C, C_1, C_2	Integration constants	---
F	Friction force	N
h	Film thickness	m
h_i	Film thickness, leading edge	m
h_o	Film thickness, trailing edge	m
h_m	Maximum height when $dp/dx=0$	m
K	Film ratio h_i / h_o	---
L	Pad length	m
P	Pressure	N/m^2



Q	Lubricant flow rate	m ³ /s
u,U,V	Sliding velocity	m/s
W	Load carrying capacity	N
η	Dynamic viscosity	Kg/m.s
τ	Shear stress	N/m ²

Acknowledgment

I would like to acknowledge Dr. Shaker Sakran Hassan (the support is gratefully acknowledged).

I also would like to acknowledge the staff of Mechanical Engineering Department / University of Technology and the people who helped me (thank you very much).

References

- [1] G. W. Stachowiak, "How tribology has been helping us to advance and to survive," *Friction*, vol. 5, no. 3, pp. 233–247, 2017, doi: 10.1007/s40544-017-0173-7.
- [2] A. Rosenkranz, P. G. Grützmacher, C. Gachot, and H. L. Costa, "Surface Texturing in Machine Elements – A Critical Discussion for Rolling and Sliding Contacts," *Adv. Eng. Mater.*, vol. 21, no. 8, pp. 1–20, 2019, doi: 10.1002/adem.201900194.
- [3] Z. Liming, L. Yongyao, W. Zhengwei, L. Xin, and X. Yexiang, "A review on the large tilting pad thrust bearings in the hydropower units," *Renew. Sustain. Energy Rev.*, vol. 69, no. September, pp. 1182–1198, 2017, doi: 10.1016/j.rser.2016.09.140.
- [4] V. Arumugaprabu, T. J. Ko, S. Thirumalai Kumaran, R. Kurniawan, and M. Uthayakumar, "A brief review on importance of surface texturing in materials to improve the tribological performance," *Rev. Adv. Mater. Sci.*, vol. 53, no. 1, pp. 40–48, 2018, doi: 10.1515/rams-2018-0003.
- [5] Zeng, F., Cheng, Y., Wan, Z., Long, Z., Zhang, Z., and Tang, Y. (July 29, 2021). "Tribological Performance of Circular-Concave-and-Spherical-Convex Compound Texture Under Hydrodynamic Lubrication." *ASME. J. Tribol.* April 2022; 144(4): 041805. <https://doi.org/10.1115/1.4051732>
- [6] Niu, Y., Hao, X., Xia, A. et al. Effects of textured surfaces on the properties of hydrodynamic bearing. *Int J Adv Manuf Technol* 118, 1589–1596 (2022). <https://doi.org/10.1007/s00170-021-08022-1>
- [7] Kumar, M., Tyagi, R. Tribological Performance of Bearing Steel with Bi-triangular and Circular Textures under Lubricated Sliding. *J. of Materi Eng and Perform* (2022). <https://doi.org/10.1007/s11665-021-065>.
- [8] A. Rosenkranz, H. L. Costa, M. Z. Baykara, and A. Martini, "Synergetic effects of surface texturing and solid lubricants to tailor friction and wear – A review," *Tribol. Int.*, vol. 155, 2021, doi: 10.1016/j.triboint.2020.106792.
- [9] H. Yue, J. Deng, D. Ge, X. Li, and Y. Zhang, "Effect of surface texturing on tribological performance of sliding guideway under boundary lubrication," *J. Manuf. Process.*, vol. 47, no. September, pp. 172–182, 2019, doi: 10.1016/j.jmapro.2019.09.031.
- [10] K. Yagi, H. Sato, and J. Sugimura, "On the magnitude of load-carrying capacity of textured surfaces in hydrodynamic lubrication," *Tribol. Online*, vol. 10, no. 3, pp. 232–245, 2015, doi: 10.2474/trol.10.232.



- [11] Y. Wang, Y. Liu, Z. Wang, and Y. Wang, "Surface roughness characteristics effects on fluid load capability of tilt pad thrust bearings with water lubrication," *Friction*, vol. 5, no. 4, pp. 392–401, 2017, doi: 10.1007/s40544-017-0153-y.
- [12] L. Shi, W. Wei, T. Wang, Y. Zhang, W. Zhu, and X. Wang, "Experimental investigation of the effect of typical surface texture patterns on mechanical seal performance," *J. Brazilian Soc. Mech. Sci. Eng.*, vol. 42, no. 5, pp. 1–12, 2021, doi: 10.1007/s40430-020-02318-1
- [13] K. Dingui, N. Brunetière, J. Bouyer, and M. Adjemout, "Surface texturing to reduce temperature in mechanical seals," *Tribol. Online*, vol. 15, no. 4, pp. 222–229, 2021, doi: 10.2474/trol.15.222.
- [14] C. Gu, X. Meng, Y. Xie, and D. Zhang, "The influence of surface texturing on the transition of the lubrication regimes between a piston ring and a cylinder liner," *Int. J. Engine Res.*, vol. 18, no. 8, pp. 785–796, 2017, doi: 10.1177/1468087416673282.
- [15] D. Gropper, T. J. Harvey, and L. Wang, "Numerical analysis and optimization of surface textures for a tilting pad thrust bearing," *Tribol. Int.*, vol. 124, pp. 134–144, 2018, doi: 10.1016/j.triboint.2018.03.034.
- [16] Zhang, Xiaohan "An Analysis of Surface Roughness and its Influence on a Thrust Bearing," *J. Phys. Ther. Sci.*, vol. 9, no. 1, pp. 1–11, 2018, [Online]. doi.org/10.1016/j.humov.2018.08.006.
- [17] K. Maharshi, T. Mukhopadhyay, B. Roy, L. Roy, and S. Dey, "Stochastic dynamic behaviour of hydrodynamic journal bearings including the effect of surface roughness," *Int. J. Mech. Sci.*, vol. 142–143, pp. 370–383, 2018, doi: 10.1016/j.ijmecsci.2018.04.012.
- [18] Kingsbury Inc., "A general guide to the principles, operation and troubleshooting of hydrodynamic bearings," 2019.
- [19] Gwidon Stachowiak ,Andrew Batchelor, " Engineering Tribology 4th Edition". ISBN: 9780128100318. Butterworth Heinemann. September 2013.
- [20] Muhannad M. Mrah " Studying The Tribological Characteristics Of Synthetic Oils Using Manufactured Inclined Bearing". Thesis, University of Technology, Iraq, 2022.
- [21] Yasir Akram Abd Al - Rida, " Study the Influence of the Triangular Slots on the Lubrication Characteristics in the Inclined Slider Bearing ", Master thesis, University of Technology, Department of Mechanical Engineering, 2011
- [22] E-radionica.com, "Pressure Sensor MPS20N0040D-S_datasheet," pp. 13, [Online]. Available: <https://datasheet4u.com/datasheet-pdf/ETC/MPS20N0040D-S/pdf.php?id=996460>
- [23] D. Gropper, L. Wang, and T. J. Harvey, "Hydrodynamic lubrication of textured surfaces: A review of modeling techniques and key findings," *Tribol. Int.*, vol. 94, pp. 509–529, 2016, doi: 10.1016/j.triboint.2015.



دراسة تأثير الأخاديد السطحية في التزيت الهيدروديناميكي تجريبياً

مهند محسن مراح عمار سليم حميد مرزه

قسم الهندسة الميكانيكية، الجامعة التكنولوجية، بغداد، العراق

* me.19.23@grad.uotechnology.edu.iq

الخلاصة

يهدف هذا البحث إلى دراسة تأثير الأخاديد المستطيلة على توزيع الضغط في محمل منزلق مائل. تم حساب تدرج الضغط في لوح سائل أحادي البعد نظرياً باستخدام معادلة رينولدز. تمت مقارنة النتائج العملية بواسطة المحمل الانزلاقي المائل، حيث قام الباحث بتصنيع وتطوير الجهاز عن طريق إضافة مستشعرات الضغط على طول الوسادات. تم إنشاء أربع وسادات بعرض فتحات مختلفة (3، 5، 8 مم) وبعمق 2 مم، واحدة بدون أخاديد وثلاث مع أخاديد مستطيلة. فحص هذا البحث عوامل مختلفة، بما في ذلك سرعات الانزلاق، وقيم ميل الوسادة، ودرجات حرارة الزيت. أشارت الاستنتاجات إلى أن توزيع ضغط النموذج المسطح يتفوق بشكل كبير على نماذج الفتحات بنسب 0.5% و 4.2% و 14% على التوالي. أحد الاستنتاجات المهمة للنماذج ذات الفتحات هو أنه كلما زاد الميل، يبدأ أقصى ضغط هيدروديناميكي في التحرك نحو بداية الوسادة. وبالتالي، يمكن استخدام النماذج المحززة في التطبيقات التي تحتاج إلى حمولة ووزن أقل. تم إجراء مقارنات تجريبية بين العمل الحالي والعمل السابق (فقط في السلوكيات). كانت عينة المقارنة مسطحة. أشارت النتائج إلى أن المستشعرات تنتج مستويات ضغط أعلى من أنابيب المانومتر في نفس ظروف التشغيل.

الكلمات الدالة: الترابولوجي، الأخاديد السطحية، المحمل المائل، التزيت الهيدروديناميكي، توزيع الضغط.

مجلات جامعة بابل
1995